

PAPER • OPEN ACCESS

Analysis of synthesized non-Gaussian excitations for vibration-based fatigue life testing

To cite this article: Marco Troncosi and Emanuele Pesaresi 2019 *J. Phys.: Conf. Ser.* **1264** 012039

View the [article online](#) for updates and enhancements.



IOP | ebooks™

Bringing you innovative digital publishing with leading voices to create your essential collection of books in STEM research.

Start exploring the [collection](#) - download the first chapter of every title for free.

Analysis of synthesized non-Gaussian excitations for vibration-based fatigue life testing

Marco Troncossi, Emanuele Pesaresi

DIN – Dept. of Engineering for Industry of the University of Bologna (Italy)

marco.troncossi@unibo.it , emanuele.pesaresi2@unibo.it

Abstract. Certain applications require that some critical components must undergo qualification tests to check their suitability with respect to vibration excitations. Measured field data are commonly considered as reference for the synthesis of random stationary signals used as excitations for shakers. The current procedures usually generate test profiles in terms of PSD, corresponding to random processes with Gaussian probability distribution of values. Such signals may be unrealistic in representing the characteristics of the reference data if the latter are not Gaussian. The Kurtosis parameter is often used to synthetically represent the amount and the amplitude of signal peaks. Its value is 3.0 for Gaussian signals, whereas higher values hold for signals featuring high peaks, e.g. due to micro-shocks. In case of accelerated fatigue life tests, the synthesized signal must induce, in a limited duration, the same fatigue damage which the reference signal cause on the component throughout its expected lifetime. The Fatigue Damage Spectrum (FDS) is generally used to quantify the fatigue damage potential associated with the excitation. The test signal is synthesized targeting the same FDS of the reference profile. This paper presents two kurtosis-control algorithms of signal synthesis in combination with a technique able to match the prescribed FDS.

1. Introduction

A common source of failure of mechanical systems operating in many applications (e.g. Automotive and Aerospace) is due to high-cycle fatigue induced by vibrations. To ensure that the most critical components work properly during their service life, vibration qualification tests are often prescribed. The so-called *Test Tailoring* procedures, now largely preferred to general Standards (e.g. MIL STD 810F, GAM EG13), require the proper definition of the test profiles (*Mission Synthesis*) to be used as vibratory excitations provided by shakers to the device under test (DUT).

The synthesis is performed starting from field data, measured for typical operational conditions of the components, aiming to reproduce their most important characteristics in laboratory tests. Instead of replicating the waveforms of the measured field data, which would result in stochasticity being lost, the conventional Mission Synthesis procedures implemented so far [1] generate the test profile in terms of a Power Spectral Density (PSD). The physical motion is obtained by applying the Inverse Fast Fourier Transform (IFFT) in combination with randomized IFFT phases generated as uniformly distributed random variables. Hence, the probability distribution of the synthesized signals is Gaussian. This could compromise the reliability of tests since most real applications feature non-Gaussian distributions. A parameter that accounts for deviations from the Gaussian law is the so-called *kurtosis* [2]: for Gaussian signals its theoretical value amounts to 3, whereas if peaks and bursts are



present (e.g. due to micro-collisions) it keeps higher values (Leptokurtic signals). The so-called kurtosis-control methods have recently gained increasing interest: their aim is to control both the PSD and the kurtosis value of the synthesized signals, in order to finally carry out more realistic tests by preserving the nature (i.e. the peaks and bursts) of real-life random excitations. In the literature, several kurtosis-control algorithms have been proposed [3-11] but not all of them prove effective in transferring peaks and bursts to the DUT. In fact, the response of a lightly damped system to an excitation may tend to Gaussian due to a filtering effect [12-14], often referred to as Papoulis' Rule. Hence, in such an instance, the DUT response is not actually different from a Gaussian signal test.

In accelerated fatigue life tests the fatigue damage induced by real-life vibrations, and accumulated by the components throughout its entire life-cycle, should be replicated on the DUT in a shorter time. The fatigue damage potential associated with a vibratory excitation is estimated via a function called Fatigue Damage Spectrum (FDS) [15]. The FDS is computed from the responses to the excitation of many Single-Degree-of-Freedom (SDOF) linear systems with natural frequencies ranging in the bandwidth of interest. The current procedures permit the synthesis of a PSD from prescribed FDS and duration of the test [1], thus leading to tests with a Gaussian input, possibly suffering from poor reliability due to the above mentioned criticalities.

Two novel kurtosis-control algorithms were proposed in [16] and it was shown that they do not suffer from Papoulis' Rule if their setup parameters are properly chosen. In this work, the algorithms are investigated further analyzing the sensitivity of their results to the setup parameters and supporting their suitability for accelerated fatigue life tests if the filter proposed by Kihm *et al.* [17] is properly implemented. The different potentialities of the algorithms are finally discussed for practical use.

2. Theoretical background

2.1 Kurtosis control algorithms

Two novel numerical algorithms have been recently proposed by the authors (comprehensively described in [16]) with the aim to synthesize a vibratory profile with the same PSD and kurtosis value of a certain reference signal. In this paper the focus is placed on their implementation, in particular on the sensitivity of final outcomes to the values of their setup parameters. Hence, the algorithms are briefly recalled in the present Section to introduce the parameters and illustrate their meaning.

The algorithm named as Multi-Level Variance (MLV) algorithm manages to make the synthesized signal reach the prescribed PSD and kurtosis value by concatenating n_b signal-blocks having the same PSD but different variance. The variance σ_i^2 of the i^{th} block is related to the overall variance σ_{tot}^2 via the following equation:

$$\sigma_{tot}^2 = \frac{1}{n_b} \sum_{i=1}^{n_b} \sigma_i^2 \quad (1)$$

The n_b levels of variance are generated randomly complying with Eq.(1) along with the constraint for the signal kurtosis value k_{tot} :

$$k_{tot} = \frac{\sum_{i=1}^{n_b} k_i \cdot \sigma_i^4}{n_b \cdot \sigma_{tot}^4} \quad (2)$$

In Eq. (2), k_i is the kurtosis value of the i^{th} block, and since the blocks are (approximately) Gaussian, its value is (approximately) equal to 3.

The inputs of the algorithm are the following:

- 1) duration of the signal to be synthesized, T ;
- 2) sampling frequency of the signal to be synthesized, F_s ;
- 3) reference vibratory profile (or, alternatively, a target PSD profile and a target kurtosis value);
- 4) ratio between the minimum standard deviation of the blocks (σ_{min}) and the overall standard

deviation σ_{tot} of the reference signal: $r_\sigma = \frac{\sigma_{min}}{\sigma_{tot}}$. It results: $0 < r_\sigma \leq 1$. Setting this parameter close to zero would lead to synthesized signals with highly variable variance over time, whereas the opposite is true if set closer to 1;

- 5) duration of the blocks of the signal, T_b ;
- 6) number of distinctive bursts that the synthesized signal should present, n_p .

The MLV algorithm leads to identical results to those obtained via the renowned technique of signal modulation. This approach consists in modulating a Gaussian signal $x(t)$ having the desired PSD with an appropriate function $w(t)$ as in the following equation:

$$y(t) = w(t)x(t) \tag{3}$$

in order to obtain a Leptokurtic signal with a desired kurtosis value [15, 18]. This method is effective in transferring the kurtosis value to the response of the DUT if the signal bursts of the modulating signal have greater duration than the inverse of the bandwidth of the lightly damped system [15]. In the case of the MLV algorithm, the Gaussian signal $x(t)$ is simply obtained by the IFFT of the reference PSD with randomly generated harmonic phases, having standard deviation equal to σ_{tot} , whereas the modulating function $w(t)$ can be expressed as:

$$w(t) = \begin{cases} \frac{\sigma_1}{\sigma_{tot}} , & 0 \leq t < T_b \\ \vdots & \\ \frac{\sigma_i}{\sigma_{tot}} , & (i - 1) \cdot T_b \leq t < i \cdot T_b \\ \vdots & \\ \frac{\sigma_n}{\sigma_{tot}} , & (n - 1) \cdot T_b \leq t < n \cdot T_b = T \end{cases} \tag{4}$$

The concatenated signal blocks are then smoothed by interpolation at the points close to the edges in order to remove the discontinuities.

The blocks generated by the MLV algorithm have the same PSD shape, but different energy (i.e. variance). This could be a limitation because signals measured in real applications (hereinafter called reference signals) often exhibit variations of the PSD shape over time [16]. In fact, some parts of the signal (i.e. blocks) could be narrow-banded, hence components having a natural frequency contained in that band could be led to resonance. This important characteristic was sought after in the development of the so-called Variable Spectral Density (VSD) algorithm, still devised to synthesize a vibratory profile whose kurtosis and PSD match the reference input ones. The VSD algorithm manages to achieve this target by concatenating n_b Gaussian blocks featuring different PSDs. The PSD variation over time is obtained by an algebraic manipulation of a matrix made of n_b columns, each one containing the PSD (periodogram) of the corresponding block. The numerical algorithm initially sets a matrix that contains the same periodogram in each block, imposed equal to the reference PSD:

$$[G'_{ij}] = \begin{bmatrix} G_1 & G_1 & \cdots & G_1 \\ \vdots & \vdots & \ddots & \vdots \\ G_{N_h} & G_{N_h} & \cdots & G_{N_h} \end{bmatrix} \tag{5}$$

where N_h is the number of harmonics of the periodogram of each block. The matrix $[G'_{ij}]$ is then manipulated to obtain the general form

$$[G''_{ij}] = \begin{bmatrix} G_{11} & G_{12} & \cdots & G_{1n_b} \\ \vdots & \vdots & \ddots & \vdots \\ G_{N_h1} & G_{N_h2} & \cdots & G_{N_hn_b} \end{bmatrix} \tag{6}$$

by performing many subsequent operations on each row, the first of which leads the generic i^{th} row to take the form:

$$[G_i \cdots pG_i \cdots [1 + (l-1)(1-p)]G_i \cdots pG_i \cdots G_i] \quad (7)$$

where $p \in [0,1]$ and l is a positive integer such that $l \leq n_b$. The algorithm iterations are fully described in [16] where it is shown that the PSD constraint is still respected if the terms of the type pG_i are $l-1$. The focus, here, is intended to be placed on two main aspects: the values of l are randomly generated throughout the iterations (still complying with some constraints) and p is an input parameter that must be set by the user. As it will also be proven later, the lower the values of p the more narrow-banded the generated blocks; this implies a greater variability of the RMS over time. Also for this algorithm, the last step consists in smoothing the transitions between consecutive blocks by interpolation, in order to remove the discontinuities due to their concatenation.

2.2 Accelerated fatigue life tests

In general, the fatigue damage potential (estimated through the spectral function FDS) associated with the signals synthesized by the MLV and VSD algorithms differs from the reference one. Therefore, if the target of the Mission Synthesis procedure is to provide input profiles for accelerated durability tests, a further correction is required. In order to adjust the FDS of the synthesized signals to match the reference one, the filtering technique described in [17] can be adopted. The steps of the procedure are briefly reported:

- 1) calculate the FDSs of the reference and synthesized signals, respectively $D_r(f)$ and $D_s(f)$;
- 2) define the spectral function (i.e. the filter): $G(f) = \left[\frac{D_r(f)}{D_s(f)} \right]^{\frac{1}{b}}$;
- 3) calculate the Inverse Fourier Transform of $G(f)$ to obtain the impulse response of the filter;
- 4) convolve the obtained impulse response with the synthesized signal.

Now the filtered synthesized signal and the reference profile have the same FDS. It should be noted that the application of the filter could generally distort the PSD and kurtosis value of the synthesized signals, to which extent will be shown and discussed in Sections 3 and 4.

3. Simulation results

Some examples of application of the two algorithms, starting from two reference profiles and setting different values of the setup parameters, are performed in order to delve into the practical impact of the user's choices. Sections 3 and 4 report the results and some discussions, respectively.

3.1 MLV simulation results: Input 1

Firstly, the MLV algorithm is applied to the reference signal of Fig. 1a, sampled at 100 Hz. The setup parameters are:

- 1) duration of the synthesized signal $T = 601.59$ s (the same as the reference signal);
- 2) output sampling frequency $F_s = 100$ Hz (the same as the reference signal);
- 3) standard deviation ratio $r_\sigma = 0.6$;
- 4) signal block duration $T_b = 2.5$ s;
- 5) number of peaks/bursts $n_p = 10$.

The probability distribution of the reference signal is Leptokurtic and kurtosis equals 6.64. By inspecting the plot of the signal (Fig. 1a) it can be seen that approximately a dozen distinctive bursts/peaks are present, hence why the parameter n_p related to the number of bursts to appear in the synthesized signal was chosen equal to 10. The value of r_σ has been chosen equal to 0.6 to give a moderate amount of variability to the RMS over time (cf. Section 2.1). The synthesized signal

(*MLV1.1*) can be seen in Fig. 1b and the PSDs of both the signals are compared in Fig. 1c in linear scale. It can be observed that they are acceptably close to each other. The statistical parameters of the reference and synthesized signals are shown in Table 1.

To have a thorough overview of the results, the responses of a SDOF system to the reference and synthesized signals are shown in Figs. 2a-b. The natural frequency of the system was set to 12 Hz, close to the peak of the PSD, and the damping ratio was arbitrarily set to 3%. The kurtosis values of the response of the SDOF system to the reference and synthesized signals are 5.82 and 5.45, respectively. One can wonder about the responses of other SDOF systems whose resonance is not excited by the excitation PSD peaks. To this aim, the responses of a series of SDOF systems with natural frequency ranging in 0-50 Hz (with 0.1 Hz resolution) were computed and the corresponding kurtosis values are plotted in Fig. 2c. This proves that even the output signals remain Leptokurtic irrespective of the DUT natural frequencies.

Another example is shown where the parameter r_σ is lowered in order to highlight how the RMS variability over time can be significantly increased. The variability is accentuated further by increasing the parameter T_b as well. In general, to make the kurtosis-control efficient at a particular angular frequency ω_n and damping ratio ζ , it is suggested that the parameter T_b be chosen greater than the inverse of the bandwidth of the system given by: $(2\zeta\omega_n)^{-1}$. Hence, the condition $T_b > (2\zeta\omega_n)^{-1}$ guarantees that, at a particular frequency ω_n and with a particular damping ratio ζ the system has enough time to respond to the bursts of the input, thus leading to a Leptokurtic output as the excitation that causes it. The setup parameters of the new run of the algorithm are the following:

- 1) $T = 601.59$ s;
- 2) $F_s = 100$ Hz;
- 3) $r_\sigma = 0.2$;
- 4) $T_b = 5$ s;
- 5) $n_p = 10$.

The synthesized signal (*MLV1.2*) is shown in Fig. 3a. It can be seen that the RMS of the n_b blocks has a higher variability over time with respect to the one shown in Fig. 1b. The PSD comparison and statistical parameters are shown in Fig. 3b and in Table 2, respectively. In Fig. 3c, the kurtosis of the responses is plotted versus the natural frequency of a series of SDOF systems in the band 5-50 Hz (with 0.1 Hz resolution and a damping ratio of 3%).

3.2. *MLV simulation results: Input 2*

The algorithm is applied to a second reference signal, sampled at 500 Hz (Fig. 4a). The input parameters are:

- 1) $T = 287$ s (the same as the reference signal);
- 2) $F_s = 500$ Hz (the same as the reference signal);
- 3) $r_\sigma = 0.2$;
- 4) $T_b = 2.5$ s;
- 5) $n_p = 30$.

Also this second reference signal proves Leptokurtic, with the kurtosis equal to 6.47. By inspecting the plot of the signal (Fig. 4a), a greater variability over time of the variance parameter can be observed with respect to input 1 (Fig. 1a). Hence, the value of r_σ has been chosen equal to 0.2, smaller than for the first input processed by the MLV algorithm. The synthesized signal (*MLV2*) can be seen in Fig. 4b and the PSDs of the signals are plotted in Fig. 4c in linear scale. It can be observed that they are acceptably close to each other. The statistical parameters of the reference and synthesized signals are shown in Table 3. To have a thorough overview of the results, the responses of a SDOF system to the reference and synthesized signal are shown in Fig. 5a-b. The natural frequency of the system was set to 150 Hz, close to the PSD maximum, and the damping ratio was again defined at 3%. The kurtosis values of the response of the SDOF system to the reference and synthesized signals are 9.01 and 6.36,

respectively. Unlike the first input, the second reference signal causes the response of the SDOF system to have a higher kurtosis than its input, whereas the synthesized signal induces a response with a similar kurtosis value to the excitation one. This behavior is very similar or even more pronounced also for other natural frequencies of the SDOF systems (in the range 5-250 Hz with 0.5 Hz resolution), as it can be inferred from Fig. 5c.

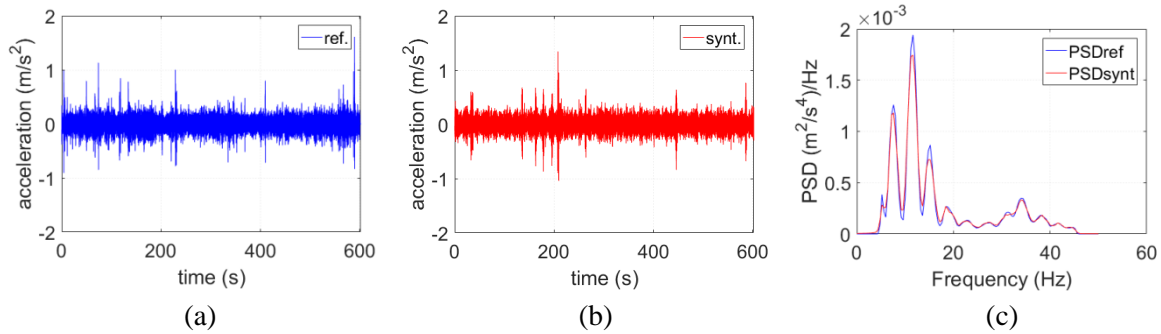


Figure 1. (a) reference signal (*Input1*); (b) synthesized signal (*MLVI.1*); (c) PSDs of the two signals.

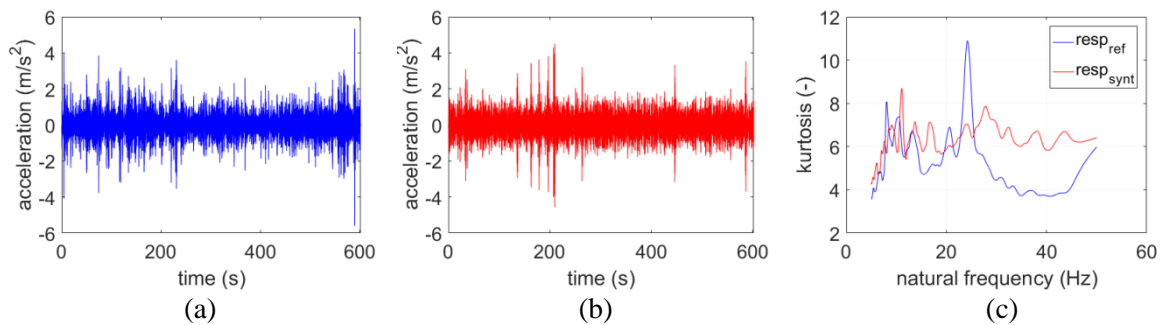


Figure 2. response of a SDOF linear system with 12 Hz natural frequency to the reference (a) and synthesized (b) signals; (c) kurtosis of the responses of a series of SDOF systems.

Table 1. Statistical parameters of the reference (Ref., *Input1*) and synthesized (Synt., *MLVI.1*) signals.

	Kurtosis (-)	Variance (m ² s ⁻⁴)	RMS (ms ⁻²)	Peak (ms ⁻²)	Crest factor (-)
Ref.	6.644	0.0125	0.1120	1.610	14.38
Synt.	6.628	0.0125	0.1120	1.343	12.00

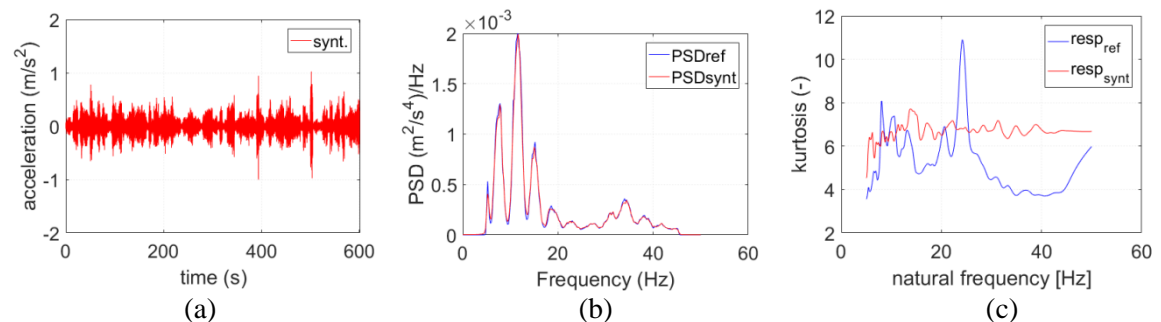
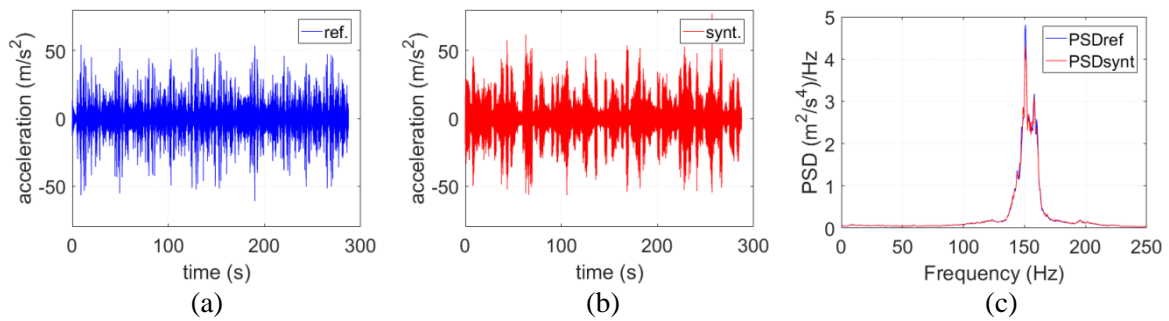
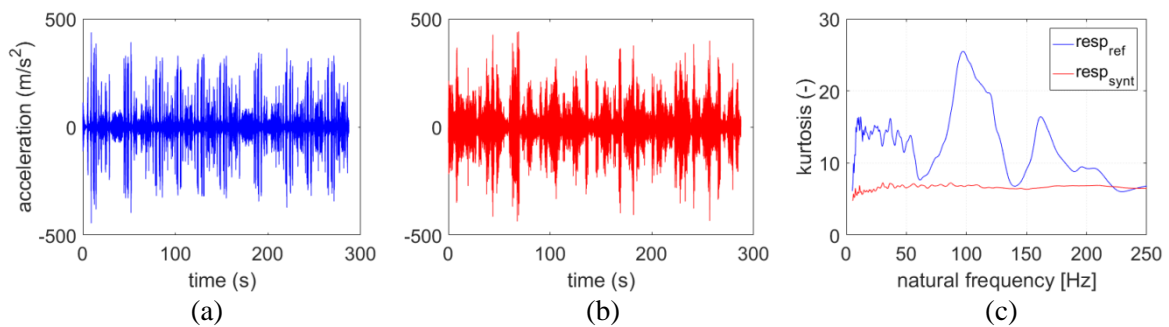


Figure 3. (a) synthesized signal (*MLVI.2*); (b) PSDs of the reference and synthesized signals; (c) kurtosis of the responses of a series of SDOF systems.

Table 2. Statistical parameters of the reference (Ref., *Input1*) and synthesized (Synt., *MLV1.2*) signals.

	Kurtosis (-)	Variance (m^2s^{-4})	RMS (ms^{-2})	Peak (ms^{-2})	Crest factor (-)
Ref.	6.644	0.0125	0.1120	1.610	14.38
Synt.	6.719	0.0125	0.1120	1.024	9.14

**Figure 4.** (a) reference signal (*Input2*); (b) synthesized signal (*MLV2*); (c) PSDs of the two signals.**Figure 5.** response of a SDOF system with 12 Hz natural frequency to the reference (a) and synthesized (b) signals; (c) kurtosis of the responses of a series of SDOF systems.**Table 3.** Statistical parameters of the reference (Ref., *Input2*) and synthesized (Synt., *MLV2*) signals.

	Kurtosis (-)	Variance (m^2s^{-4})	RMS (ms^{-2})	Peak (ms^{-2})	Crest factor (-)
Ref.	6.475	70.98	8.425	61.03	7.244
Synt.	6.467	70.98	8.425	77.40	9.186

3.3. VSD simulation results: *Input 1*

The VSD algorithm is now applied to the first reference signal of Fig. 1a. The setup parameters are:

- 1) $T = 601.59$ s;
- 2) $F_s = 100$ Hz;
- 3) $p = 0.5$.

The value of p has been chosen equal to 0.5 to give a moderate variability to the RMS over time, its meaning being similar to that of parameter r_σ but it also accounts for the extent of bandwidth variation of each signal block. The synthesized signal (*VSD1.1*) is reported in Fig. 6a. The PSDs of the signals, plotted in Fig. 6b in linear scale, are acceptably close to each other. The statistical parameters of the reference and synthesized signals are shown in Table 4. The kurtosis values of the response of SDOF systems (with natural frequencies ranging from 5 to 50 Hz) are plotted in Fig. 6c, which shows that the VSD algorithm generates signals prompting system responses with a higher kurtosis than the input.

Another example is shown where the parameter p is lowered in order to highlight how the RMS and bandwidth variability over time among the n_b signal blocks can be extremely accentuated by the VSD algorithm. The setup parameters were set as follows:

- 1) $T = 601.59$ s;
- 2) $F_s = 100$ Hz;
- 3) $p = 0.1$.

The synthesized signal (*VSD1.2*) is shown in Fig. 7a. It can be seen that its RMS has higher variability with respect to the one shown in Fig. 6a. The PSD comparison and statistical parameters are reported in Fig. 7b and in Table 5, respectively. In Fig. 7c, the kurtosis of the SDOF systems responses is plotted (natural frequency from 5 to 50 Hz with 0.1 Hz resolution and damping ratio equal to 3%).

3.4. VSD simulation results: Input 2

The reference signal of Fig. 4a is now processed by the VSD algorithm with the following parameters:

- 1) $T = 287$ s;
- 2) $F_s = 500$ Hz;
- 3) $p = 0.2$.

The synthesized signal (*VSD2*) can be seen in Fig. 8a. The PSDs and the statistical parameters of the reference and synthesized signals are reported in Fig. 8b (linear scale) and Table 6, respectively. The kurtosis of the SDOF systems responses is plotted in Fig. 8c for natural frequencies ranging from 5 to 250 Hz.

3.5. Fatigue Damage Spectrum correction

In the case of vibration testing intended to assess the fatigue life of a product, the synthesized signal is meant to induce (possibly for a short test duration) the same fatigue damage on the DUT that affects the latter throughout its expected lifetime. The FDSs of the reference and synthesized signals, representing the damage potentials associated with vibratory excitations, should match. The most important parameters involved in their computation are: Wohler's curve slope b of the DUT material, the expected lifetime (T_R) of the DUT if subjected to the reference signal, the duration (T_S) of the accelerated fatigue life test when the DUT is excited by the synthesized signal, and the damping ratio ζ of the SDOF systems. The reference and synthesized signals (with their own duration T) are considered to be consecutively replicated until T_R and T_S are reached.

In order to assess the suitability of the signals synthesized by the two algorithms to serve as input in (accelerated) fatigue life tests, their FDSs were computed and compared to the reference ones. The values chosen for this application are: $b = 5$, $\zeta = 3\%$, $T_R = 100$ h, and $T_S = 100$ h.

The test duration T_S was firstly set equal to the expected lifetime T_R , implying a non-accelerated test, in order to better compare and discuss the results. For the sake of brevity, only the processing of the synthesized signal *VSD2* of Fig. 8a is here analyzed (similar results and conclusions hold for all the signals of the former Sections), since its FDS proved to differ from the reference FDS by some orders of magnitude at certain frequencies (Fig. 9a). The matching of the two FDSs was achieved by applying the filter mentioned in Section 2.2 [17] and can be appreciated in Fig. 9b, whereas Fig. 9c and Table 7 show the (slight) discrepancy between the PSDs and statistical parameters, respectively, of the filtered (*VSD2f*) and the reference signals.

If a time reduction factor of 10 is considered ($T_R = 100$ h, $T_S = 10$ h), the FDS computed for the synthesized signal differs from the reference one to a greater extent (Fig. 10a), as expected. The effect of the filter application to adjust the fatigue damage potential of the synthesized signal is thus much more meaningful (Fig. 10b). The PSDs of the reference and the filtered signals are shown in Fig. 10c and their statistical parameters reported in Table 8. It is evident that as the test duration decreases, the filtering procedure increases the PSD of the synthesized signal, in order to achieve the FDS matching. Besides, both the statistical parameters of Table 7 and Table 8 highlight that the distribution of the signal remains Leptokurtic, with minor changes to the kurtosis values.

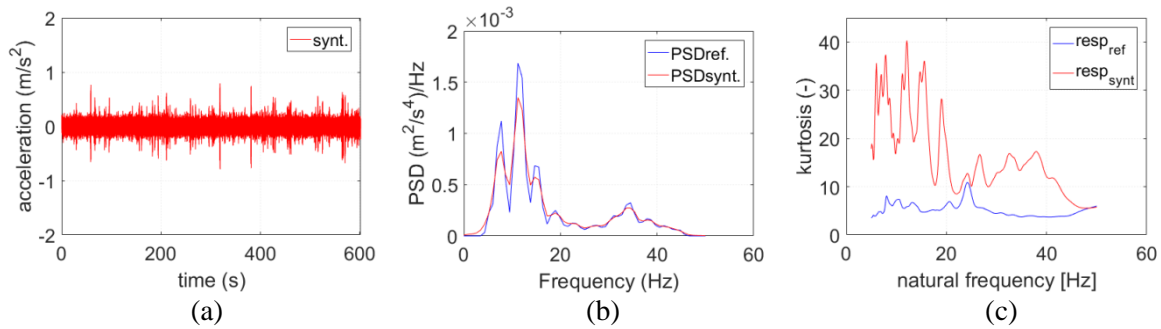


Figure 6. (a) synthesized signal (*VSD1.1*); (b) PSDs of the reference and synthesized signals; (c) kurtosis of the responses of a series of SDOF systems.

Table 4. Statistical parameters of the reference (Ref., *Input1*) and synthesized (Synt., *VSD1.1*) signals.

	Kurtosis (-)	Variance (m ² s ⁻⁴)	RMS (ms ⁻²)	Peak (ms ⁻²)	Crest factor (-)
Ref.	6.644	0.0125	0.1120	1.610	14.38
Synt.	6.669	0.0125	0.1120	0.7918	7.073

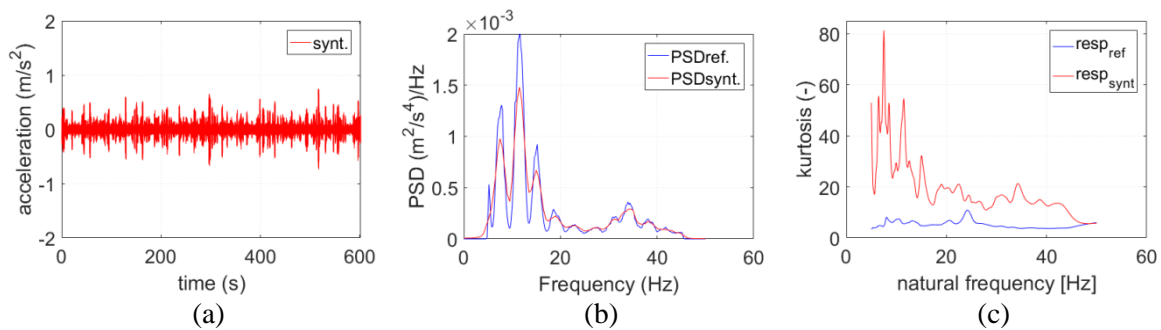


Figure 7. (a) synthesized signal (*VSD1.2*); (b) PSDs of the reference and synthesized signals; (c) kurtosis of the responses of a series of SDOF systems.

Table 5. Statistical parameters of the reference (Ref., *Input1*) and synthesized (Synt., *VSD1.2*) signals.

	Kurtosis (-)	Variance (m ² s ⁻⁴)	RMS (ms ⁻²)	Peak (ms ⁻²)	Crest factor (-)
Ref.	6.644	0.0125	0.1120	1.610	14.38
Synt.	6.651	0.0125	0.1120	0.7500	6.699

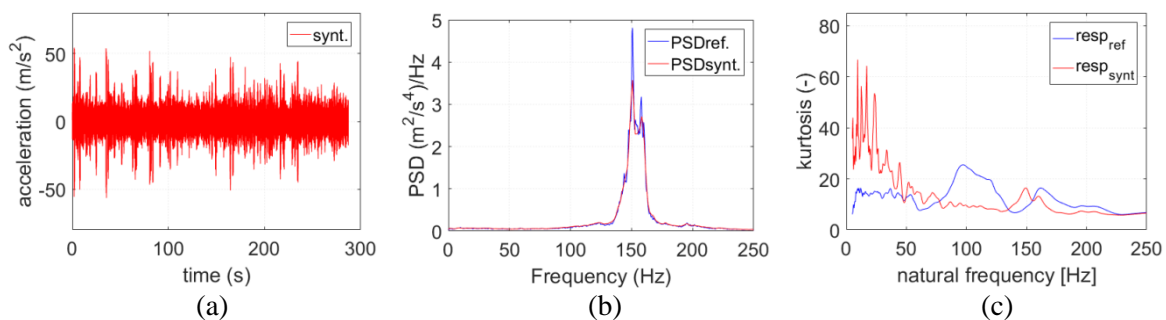
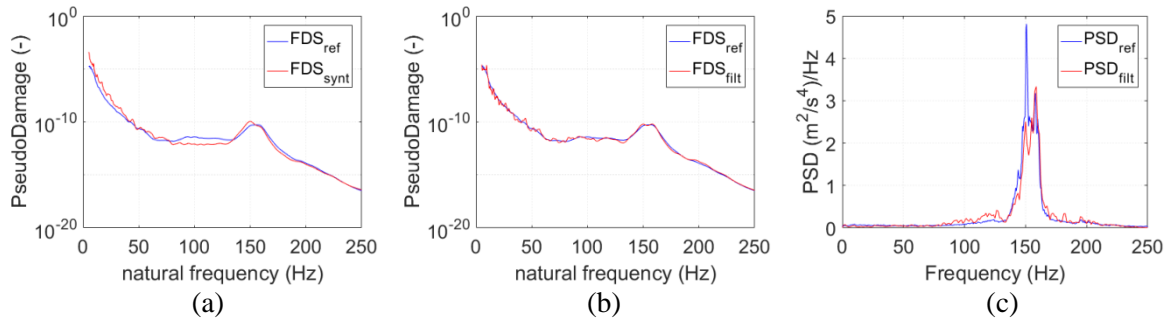


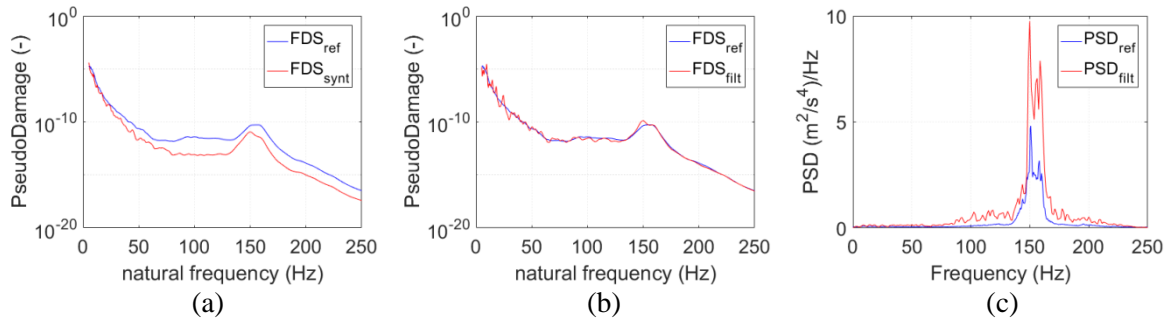
Figure 8. (a) synthesized signal (*VSD2*); (b) PSDs of the reference and synthesized signals; (c) kurtosis of the responses of a series of SDOF systems.

Table 6. Statistical parameters of the reference (Ref., *Input2*) and synthesized (Synt., *VSD2*) signals.

	Kurtosis (-)	Variance (m^2s^{-4})	RMS (ms^{-2})	Peak (ms^{-2})	Crest factor (-)
Ref.	6.475	70.98	8.425	61.03	7.244
Synt.	6.484	70.98	8.425	56.44	6.700

**Figure 9.** (a) FDSs of the reference (*Input2*) and synthesized (*VSD2*) signals; (b) FDSs of the reference and filtered (*VSD2f*) signals; (c) PSDs of the reference and filtered signals. $T_R = T_S = 100\text{h}$.**Table 7.** Statistical parameters of the reference (Ref., *Input2*) and synthesized (Filt., *VSD2f*) signals.

	Kurtosis (-)	Variance (m^2s^{-4})	RMS (ms^{-2})	Peak (ms^{-2})	Crest factor (-)
Ref. ($T_R = 100\text{h}$)	6.475	70.98	8.425	61.03	7.244
Filt. ($T_S = 100\text{h}$)	6.599	69.55	8.340	75.56	9.060

**Figure 10.** (a) FDSs of reference (*Input2*) and synthesized (*VSD2*) signals; (b) FDSs of the reference and filtered (*VSD2f*) signals; (c) PSDs of the reference and filtered signals. $T_R = 100\text{h}$, $T_S = 10\text{h}$.**Table 8.** Statistical parameters of the reference (Ref., *Input2*) and synthesized (Filt., *VSD2f*) signals.

	Kurtosis (-)	Variance (m^2s^{-4})	RMS (ms^{-2})	Peak (ms^{-2})	Crest factor (-)
Ref. ($T_R = 100\text{h}$)	6.475	70.98	8.425	61.03	7.244
Filt. ($T_S = 10\text{h}$)	6.688	180.7	13.44	100.4	7.470

4. Discussion

The results show that the MLV algorithm synthesizes signals able to transfer their Leptokurtic distribution to the response of the DUT. In particular, the kurtosis computed for the responses of the excited SDOF linear systems remains almost constant irrespective of the latter's natural frequency (Figs. 2c, 3c and 5c), with relatively small fluctuations around a value close to the excitation signal kurtosis (Tables 1-3). This can be motivated by the following reason: the blocks constituting the synthesized signal all have a wide-band PSD, so that rapid resonant effects cannot occur. The kurtosis

transfer is only due to the energy of the bursts appearing in the signal and the high excursions in the output cannot physically contain more energy. However, it should be noted that the setup parameters may significantly affect the results. In particular, if the bursts' duration is not long enough, the system may not have time to respond thus preventing high excursions to appear in the response. Therefore, the choice of the parameter T_b value is definitely relevant: if the first natural (angular) frequency ω_n and damping ratio ζ of the DUT are known, the lower limit can be assessed as $(2\zeta\omega_n)^{-1}$. The choice of the other two parameters, n_p and r_σ , strictly associated with the number and amplitudes of the bursts to appear in the synthesized signal, can be done easily by evaluating the bursts present in the reference input and replicating their characteristics. Finally, it is worth recalling that randomness in the synthesized profiles is guaranteed since the algorithm generates randomly the modulating function of Eq. (4) and manipulates deterministically the phases of only one IFFT block [16]. Different runs of the algorithm to process – with unchanged setup parameters – the same reference signal thus provide the synthesis of different profiles (all complying with the target PSD and kurtosis). Therefore random vibration tests that require a sizable duration (e.g. qualification, functional, reliability tests) can be carried out starting from short environmental measurements by concatenating many profiles synthesized by the MLV algorithm.

On the other hand, the VSD algorithm presents different qualities due to the intrinsic generation of narrow-banded signal blocks, which can exasperate resonance effects on the DUT: the lower the value of parameter p the more evident the resonance occurrence. The advantages of this algorithm are two-fold: (i) the synthesized excitations, though characterized by a relatively low crest factor, are able to generate responses with (very) high kurtosis (i.e. with high amplitude peaks) still subjecting the shaker to moderate loads; (ii) the kurtosis of the response is not constant with respect to the DUT natural frequency and is generally higher than the input kurtosis (which is a case encountered in many practical applications, due to the variable spectrogram of real-life vibrations). One limitation of the VSD algorithm could be that the PSD variation over time is intrinsically random and cannot be controlled. On the other hand, this feature adds to the signal stochasticity, which is also increased by the complete aleatory generation of the harmonic phases in the IFFT transform, for each block.

Both the kurtosis-control algorithms could lead to signals with a fatigue damage potentials very different from that of the excitation, since they do not directly control the FDS. If the Mission Synthesis is performed for durability testing purposes, the filter proposed by Kihm *et al.* [17] can be effectively applied to correct the FDS of the signals generated by both the MLV and the VSD algorithms. As shown by the two cases illustrated in Section 3.5, the new signals feature similar Leptokurtic distributions as their corresponding synthesized ones, with slight differences – due to the filter action – observed in the PSDs and the statistical parameters. The combination of the VSD algorithm with the subsequent FDS correction appears particularly promising for the synthesis of excitation signals for accelerated fatigue life tests (recalling the two above mentioned advantages).

5. Conclusion

Two novel kurtosis-control algorithms previously proposed by the authors are here discussed further. One algorithm, named Multi-Level Variance (MLV) algorithm, splits the signal to be synthesized into blocks of the same size featuring variable variance. Namely, the shape of the PSDs of each block remains the same, but the amplitudes are scaled by a proper factor. The overall PSD and kurtosis match the reference ones within a certain tolerance. The kurtosis of the response computed for many SDOF linear systems tends to be constant with respect to their natural frequencies, keeping values close to the excitation kurtosis (due to the generated signals being wide-banded in all the blocks). The peaks are thus not filtered, i.e. the problem associated with the Papoulis' Rule does not occur.

A second algorithm, named Variable Spectral Density (VSD) algorithm, splits the signal into blocks of the same size, with variable PSD. The overall PSD and kurtosis closely approach the reference ones. The kurtosis of the output proves to vary conspicuously over the natural frequency of the excited SDOF system, due to the generated signals being narrow-banded in some blocks. This behavior shows a greater resemblance to the response kurtosis of the reference signal, which is also

generally higher than that of the input excitation. Also in this case, the Papoulis' Rule does not apply.

The fatigue damage potential of the synthesized and reference signals are different, which generally occurs for any kurtosis-control algorithm as well. Such a discrepancy can be compensated for by the application of a special filter computed from the Fatigue Damage Spectra (FDS) of the synthesized and the reference signals, thus making the algorithms suitable to generate excitation profiles for accelerated fatigue life tests. Future efforts will address the simultaneous control of both FDS and kurtosis in place of the two-steps procedure adopted here.

Acknowledgments

The research is financially supported by *Easting s.r.l.s.* (Trieste, Italy) and *Dana-Rexroth Transmission Systems* (Trento, Italy), which are gratefully acknowledged.

References

- [1] Lalanne C 2009 *Mechanical Vibration and Shock Analysis-Volume 5: Specification Development* (London: John Wiley & Sons, Inc-ISTE)
- [2] Lalanne C 2009 *Mechanical vibration and shock analysis-volume 3: Random Vibration* (London: John Wiley & Sons, Inc-ISTE)
- [3] Steinwolf A 2015 Vibration testing of vehicle components by random excitations with increased kurtosis *Int. J. Vehicle Noise and Vibration* Vol 11 pp 39-36
- [4] Zhang J, Cornelis B, Peeters B, Janssens K and Guillaume P 2016 *A new practical and intuitive method for kurtosis control in random vibration testing* Procs. 27th ISMA (Leuven, Belgium)
- [5] Steinwolf A 1996 Approximation and simulation of probability distributions with a variable kurtosis value *Computational Statistics and Data Analysis* Vol 21 pp 163-180
- [6] Kihm F and Rizzi S A, Ferguson N S and Halfpenny A 2013 *Understanding how kurtosis is transferred from input acceleration to stress response and its influence on fatigue life* Procs. 11th RASD (Pisa, Italy)
- [7] Cornelis B, Steinwolf A, Troncossi M and Rivola A 2015 *Shaker testing simulation of non-Gaussian random excitations with the fatigue damage spectrum as a criterion of mission signal synthesis* Procs. ICoEV (Ljubljana, Slovenia)
- [8] Smallwood D O 2005 Generating non-Gaussian vibration for testing purposes *Sound and Vibrations* Vol 39
- [9] Winterstein S R 1988 Nonlinear vibration models for extremes and fatigue *ASCE Journal of Engineering Mechanics* Vol 114
- [10] Merritt R G 1997 *A stochastic model for the pulse method – Part 2: random part* Procs. 43rd IEST Annual Technical Meeting (Los Angeles, USA)
- [11] Minderhoud J and Van Baren P 2010 Using Kurtosion[®] to Accelerate Structural Life Testing *Sound And Vibration* Vol 44
- [12] Papoulis A 1972 Narrow-Band systems and Gaussianity *IEEE Trans. On Information Theory* Vol 18
- [13] Papoulis A 1991 *Probability, Random Variables and Stochastic Processes* (McGraw-Hill)
- [14] Van Baren J and Van Baren P 2007 *Kurtosiontm-getting the kurtosis into the resonances*, Procs. 78th SAVIAC
- [15] Lalanne C 2009 *Mechanical Vibration and Shock Analysis-Volume 4: Fatigue Damage* (London: John Wiley & Sons, Inc-ISTE)
- [16] Pesaresi E and Troncossi M 2018 *Synthesis of vibration signals with prescribed power spectral density and kurtosis value* Procs. 28th ISMA (Leuven, Belgium)
- [17] Kihm F, Halfpenny A and Munson K 2016 *Synthesis of Accelerated and More Realistic Vibration Endurance Tests Using Kurtosis* SAE Technical Paper
- [18] Kihm F, Ferguson N S and Antoni J 2015 Fatigue life from kurtosis controlled excitations *Procedia Engineering* Vol 133 pp 698-713